Cross-Diffusion Waves as a trigger for Multiscale, Multi-Physics Instabilities:Theory

Klaus Regenauer-Lieb[1], Manman Hu[2], Christoph Schrank[3], Xiao Chen[1], Santiago Peña Clavijo[1], Ulrich Kelka[4], Ali Karrech[5], Oliver Gaede[3], Tomasz Blach[1], Hamid Roshan[1], and Antoine Jacquey[6]

[1]School of Minerals and Energy Resources Engineering, UNSW, Sydney, NSW 2052 Australia
[2]Department of Civil Engineering, The University of Hong Kong, Hong Kong
[3]Science and Engineering Faculty, Queensland University of Technology, Brisbane, QLD, 4001, Australia
[4]CSIRO, ARRC Technology Park, Kensington, WA 6151, Australia
[5]School of Engineering, University of Western Australia, Crawley, WA 6009, Australia
[6]Department of Civil and Environmental Engineering, Massachusetts Institute of Technology, Cambridge, MA, USA

Correspondence: Klaus Regenauer-Lieb (regenau@gmail.com)

Abstract. We propose a non-local, meso-scale approach for coupling multiphysics processes across the scale. The physics is based on discrete phenomena, triggered by local Thermo-Hydro-Mechano-Chemical (THMC) instabilities, that cause cross-diffusion (quasi-soliton) acceleration waves. These waves nucleate when the overall stress field is incompatible with accelerations from local feedbacks of generalized THMC thermodynamic forces that trigger generalized thermodynamic fluxes of another kind. Cross-diffusion terms in the 4×4 THMC diffusion matrix are shown to lead to multiple diffusional P- and S-wave equations as coupled THMC solutions. Uncertainties in the location of meso-scale material instabilities are captured by a wave-scale correlation of probability amplitudes. Cross-diffusional waves have unusual dispersion patterns and, although they assume a solitary state, do not behave like solitons but show complex interactions when they collide. Their characteristic wavenumber and constant speed define mesoscopic internal material time-space relations entirely defined by the coefficients of the coupled THMC reaction-cross-diffusion equations. For extreme conditions, cross-diffusion waves can lead to an energy cascade connecting large and small-scales and cause solid-state turbulence.

1 Introduction

In a paper presented at the Nobel Conference XXVI, St. Peter, in Minnesota on the 2-3 Oct 1990 Ilya Prigogine proposed that systems that are pushed far from equilibrium react by forming new space/time dissipative structures that lead to internal material timescales. He goes on to suggest that incorporating these new timescales at the interface of solving the problems of the physics of the very small to the very large defines a new frontier in science.

This contribution extends on this idea in a first multi-scale and multi-physics formulation that extends the approach of coupled hydro-mechanical oscillators to a generic multiphysics approach, succinctly called "*(geo-)wave mechanics*". Specifically, we consider, without loss of generality, as examples multiphysics Thermo-, Hydro-, Mechanical- and Chemical (THMC) coupling.

2 Dissipative structures

Before discussing cross-scale coupling it is useful to briefly review insights into the formation of discrete dissipative structures. The concept was introduced first in chemical and biological systems where morphogenic patterns (Turing, 1952) were identified as solutions to the underlying reaction-diffusion equations (see Figure 1). These discrete patterns were later on named Turing patterns. A review of Turing patterns in nature can be found in Ball (2012).

We propose here a generalised approach that is known in bio-physics as taxis (Heilmann et al., 2018). For example, the pufferfish and the siltstone in Figure 1 show similar patterns caused by a fundamental mechanism known as taxis. This is a process that forces components of a pattern to organise as an ensemble in reaction to changes in the environment, and so to move towards, or away from a perturbation. The process eventually leads to the formation of a new energetically stable pattern. The fundamental pattern-forming taxis mechanism can be caused by adhesive forces (hapto-taxis), hydrodynamic (gyro-taxis), gravitational (gravi-taxis), light intensities (photo-taxis), or chemical driving forces; chemo-taxis; as shown in Figure 1. Non-biological patterns are generally formed by Thermal, Hydrodynamic, Mechanical, and Chemical (THMC) reactions, which can also include electrical and biological drivers. In mathematical biology, taxis models are used to understand and quantify a variety of complex problems, ranging from nerve pulse responses and spreading of diseases (Zemskov et al., 2017) to predicting the Spatio-temporal patterns of predator-prey systems.

However, except for the seminal early work by Ortoleva and co-workers (Dewers and Ortoleva, 1990; Ortoleva, 1993, 1994) developments of taxis models in Earth and Material Sciences have lagged. A review of the progress made in this field as well as a specific case study of rhythmic banding in marls can be found in the recent work of L'Heureux (L'Heureux, 2018; L'Heureux, 2013). The present work develops the key ideas into a geomechanical perspective building on an initial approach proposed for hydro-mechanical coupling (Hu et al., 2019; Alevizos et al., 2017; Regenauer-Lieb et al., 2016; Veveakis and Regenauer-Lieb, 2015; Regenauer-Lieb et al., 2013).

Since the early work in the 1990's (Ortoleva, 1994) the impact of experimental, numerical, and theoretical studies on multi-physics and multiscale framework for Earth Sciences has been sparse. The current practice is to still use engineering solutions based on empirical material laws to address specific natural and engineering problems in geological systems and energy production (such as geothermal energy, nuclear waste disposal, reservoir engineering for oil and gas, the formation of mineral deposits, induced seismicity, natural hazards, and CO_2 sequestration and utilization). These empirical engineering approaches are often inadequate, as indicated, for example, in the failure to avoid the 5.5 magnitude earthquake in Pohang Korea in November 2017, which was anthropogenically induced by high-pressure hydraulic injection during the previous two years (Grigoli et al., 2018).

By analogy to the mathematically similar biological and chemical systems we propose here that earthquake instabilities are preceded by propagating THMC dissipative waves which could enable new detection methods if they can be resolved by sensors. In chemical systems, propagating waves stemming from reaction-diffusion physics, are very well documented and the postulate here is that this applies generally to all THMC coupled processes. Excellent update of the formulation for chemical systems can be found in Vanag and Epstein (2009). While chemical oscillations thus appear to be well understood, the

Figure 1. Dissipative patterns in chemical and biological systems: Simulated and real patterns on Puffer Fish (Sanderson et al., 2006) and strangely patterned siltstone (Zebra Rock, Ranford formation in the Kununurra district in the East Kimberley region of Western Australia). Both pattern formations can be modelled by a reaction-diffusion-advection type instability due to chemo-taxis.

55 phenomenon of an oscillatory response is less well established in other THMC systems. However, these systems show the same transitions from a simple continuum response to a highly localized state. The existence of a discrete, particle-like nature has also been discovered in fluids when they are driven far from equilibrium. If driven far from equilibrium by surface forces, fluids clearly show (see Fig. 3) a highly dissipative, sharp transition from a continuum state to one of a highly localized, propagating, particle-like state (Lioubashevski et al., 1996). For the case of deforming geomaterials localization phenomena, characterized

60 by a sudden transition from continuum deformation behaviour to a highly localized state, are also well established in solid mechanics applications (Rudnicki and Rice, 1975). However, direct experimental evidence for precursory transient travelling solitary states is largely unknown and has only been postulated recently based on mathematical considerations (Hu et al., 2019). The lack of experimental evidence is due to the large length scale of the geomechanical phenomena and the long-time scales of observation required to mimic natural processes in the laboratory.

65   The dynamics of the formation of these mechanical dissipative patterns can therefore only be investigated using analogue materials in the laboratory. Analogue experiments have been performed in a granular, brittle- matter compressed in a uniaxial direction (Guillard et al., 2015; Einav and Guillard, 2018). A propagating compaction wave phenomenon has been observed. Acoustic bursts have been registered when the waves interact with interfaces leading to the conversion of their kinetic energy into acoustic emissions. The phenomenon has been compared to ice-quakes in ice sheets (Einav and Guillard, 2018). While

70 these experiments allow some insight into the precursor phenomena of stationary compaction bands the experiments themselves never reached the stationary mode. This aspect will be discussed in more detail in part 2 (Regenauer-Lieb et al., 2020) where experiments that are very close to the stationary mode are also introduced (Barraclough et al., 2017). The stationary mode allows development of a robust *thermomechanics* theory which offers a modular thermodynamically self-consistent approach for modeling earth instabilities (Jacquey and Regenauer-Lieb, 2020).
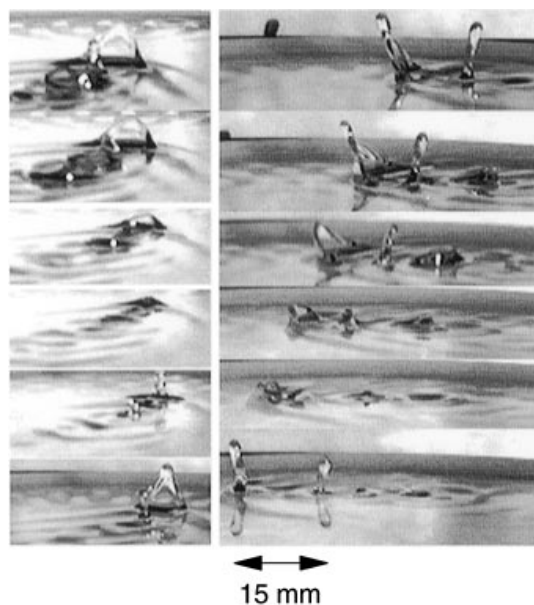
Figure 2. Dissipative patterns in fluid systems: Water molecules exhibit a discrete quantum-like solitary state when forced by a mechanical shaker at a critical condition (here 41 Hz). Periodic finger-like solitary states travel from right to left at a constant velocity. Each snapshot shows 20 ms intervals. Unlike classical solitons their appearance is particle-like. They can pass through each other with a slight loss of amplitude, or 'collide' to create a new state whose direction of propagation is at an angle to that of the original states or disintegrate upon collision (image from ref (Lioubashevski et al., 1996)).

75   Experiments with highly porous carbonates have been performed (Chen et al., 2020). These produced stationary and non-stationary compaction bands under uniaxial loading. Unfortunately, these experiments have the opposite problem in that the exact analysis of the dynamic evolution did not reach sufficient resolution in space and time to convincingly detect the wave phenomenon described in the granular brittle matter. We, therefore, explore in this contribution theoretical predictions of the dynamic wave propagation based on an extension of the *thermomechanics* approach for wave propagation in dissipative
80   materials (Coleman et al., 1965). We call this extension *(geo-)wave mechanics* due to its mathematical similarity with quantum physics approaches.

     We propose here that the dissipative wave phenomenon is universal for THMC reaction-diffusion systems that are driven far from equilibrium. The approach allows an interpretation of observations in nature and the laboratory in terms of propagating particle-like states which emerge as stationary Turing patterns for long-timescale standing wave solution of a THMC cross-
85   diffusion formulation. In order to recover the dissipative wave equations, we present in the following the standard constitutive assumptions for any generic thermodynamic fluid or solid mechanical system and describe how the physics of THMC feedbacks can be implemented to resolve the phenomenon of propagating dissipative waves in these systems.

Figure 3. Dissipative patterns in solid systems: Two generations of compaction and shear enhanced compaction bands (hand lense for scale) in silt- and sandstones of the Miocene Whakataki formation, south of Castlepoint, North Island, New Zealand. The porosity reduction renders the bands less susceptible to erosion causing a marked positive relief. The periodic bands reminiscent of a standing wave phenomenon are thought to be the result of slow compression of the porous siltstone in the compressive environment (accretionary wedge) of the Hikurangi subduction zone.

3 Wave equations

3.1 Constitutive assumptions

90 The fundamental equation of motion is:

$$\nabla \cdot \boldsymbol{\sigma} + \rho \mathbf{f} = \rho \mathbf{a}, \tag{1}$$

where $\boldsymbol{\sigma} = \sigma_{ij}$ is the Cauchy stress tensor, ρ the density, $\mathbf{f}$ is a body force (e.g. gravity) and $\mathbf{a}$ the acceleration. This equation does not stipulate a constitutive law but with constitutive assumptions it becomes the master equation for the theory of elastic waves, fluid mechanics and continuum mechanics. In elasticity, wave equations directly result from the equation of motion

95 defining the wave characteristics by using the Helmholtz decomposition, in terms of shear (S-wave) and compressional (P-wave) wave velocities which is a convenient description for the purpose of this paper.

For an isotropic elastic medium, for instance, accelerations in Eq. (1) are only allowing elastic displacements described by $\mathbf{u}$. In this case the material can be characterized by just two velocities: the elastic P-wave velocity v_p and the elastic S-wave

velocity v_s, and we obtain from Eq. (1) the elastic-wave equation:

100
$$\frac{\partial^2 \mathbf{u}}{\partial t^2} = \underbrace{v_p^2 \nabla(\nabla \cdot \mathbf{u})}_{P \text{ wave}} - \underbrace{v_s^2 \nabla \times (\nabla \times \mathbf{u})}_{S \text{ wave}}. \tag{2}$$

Similarly, by allowing the material to deform in a viscous manner, acceleration can be monitored by a local change in velocity $\mathbf{v}$, and the Helmholtz decomposition identifies a scalar P-wave and a vectorial S-wave potential field. The material constants are the dynamic shear η and bulk ζ viscosities to obtain the generalized Navier-Stokes equation:

$$\rho \left(\frac{\partial \mathbf{v}}{\partial t} + \mathbf{v} \cdot \nabla \mathbf{v} \right) = -\nabla p + 2\nabla^2(\eta \dot{\boldsymbol{\epsilon}}') + \nabla(\zeta(\nabla \cdot \mathbf{v})) + \rho \mathbf{f} \tag{3}$$

where $\mathbf{I}$ is the identity matrix and

$$\dot{\boldsymbol{\epsilon}}' = \frac{1}{2} \left(\nabla \mathbf{v} + (\nabla \mathbf{v})^T \right) - \dot{\boldsymbol{\epsilon}}_0$$

is the deviatoric viscous strain-rate. with

$$\dot{\boldsymbol{\epsilon}}_0 = \frac{1}{3}(\nabla \cdot \mathbf{v})\mathbf{I}$$

105   We emphasize here, that although the Helmholtz decomposition can be performed in a similar way to derive volumetric and shear moduli that describe dissipative material behaviour, their response to infinitesimal perturbation is generally to dampen propagating elastic waves. One could, therefore, come to the erroneous conclusion that their contribution to precursory wave phenomena to macroscopic failure is an overall suppression of instabilities.

Coleman and Gurtin (1965) have shown that this conclusion is wrong using the concept of materials with fading memory con-
110   ceptualized by rational thermodynamics. We are using a simpler approach and are introducing fading memory through THMC dissipation processes based on the non-equilibrium thermodynamics approach of deGroot (1962). Therein, non-equilibrium conditions are seen as a concatenation of thermostatic equilibrium processes. We, therefore, can use the local equilibrium definition of the pressure as $p = -\frac{\partial U}{\partial V}$, where U is the internal energy and V the volume and explore the emergent dynamics through investigating the stability of small perturbations from individual equilibrium states. In the present context pressure is
115   therefore defined as $p = \frac{1}{3} tr(\boldsymbol{\sigma})$ and is negative for compression.

For the elasto-visco-plastic case, we have the equivalent fourth-order elastic-viscoplastic stiffness tensor $\mathbf{C}$ characterizing material stiffness and the corresponding elastic-viscoplastic bulk viscosity ζ to give

$$\rho \left(\frac{\partial \mathbf{v}}{\partial t} + \mathbf{v} \cdot \nabla \mathbf{v} \right) = -\nabla p + 2\nabla(\boldsymbol{C} \dot{\boldsymbol{\epsilon}}') + 3\nabla(\zeta \dot{\epsilon}_0) + \rho \mathbf{f}, \tag{4}$$

in this case $\dot{\boldsymbol{\epsilon}}'$ denotes the deviatoric elastic-visco-plastic strain-rate and $\dot{\epsilon}_0$ the equivalent volumetric strain-rate. While the
120   emergence of elastic $P-$ and $S-$ waves for any infinitesimal disturbance is a well-known physics phenomenon, dissipative processes are commonly known to dampen elastic waves. Long-range wave propagation in dissipative materials was therefore contested for a long time (Coleman and Gurtin, 1965). Ideal elastic waves without damping propagate without loss of energy as they are based on the conservation of energy. However, the dissipative chemical and biological diffusion waves are known to propagate as autonomous wave sources, spontaneous oscillations, and quasi-stochastic waves which are synchronized over
125   the entire space to form dissipative structures (Vasil'ev, 1979).

They are an entirely different class of waves as they are based on dissipation in active kinetic systems in contrast to waves in conservative systems. For simplicity, we only discuss the slow visco-plastic wave phenomenon allowing the investigation of conservative and dissipative waves as different processes. For decoupling elastic and dissipative waves, we need to assume large differences in the propagation speed of the waves. This is done by assuming Maxwellian rheology, implying a separation of

130   elastic and visco-plastic wave time-scales in the context of an additive strain-rate decomposition of Eq. (2) and (4). To recover dissipative waves from the above discussed Navier-Stokes equation, modified for the inclusion of elastoplastic behaviour, we introduce local thermodynamic THMC feedback processes that change the instantaneous fourth-order elastic-visco-plastic stiffness tensor $\mathbf{C}$.

3.2   Acceleration waves and classical theories of localisation

135   The simplest implementation of the non-equilibrium approach of deGroot (1962) is the theory of internal variable thermodynamics which unifies the kinetic description of chemical reaction-diffusion processes and the above described elastic-viscoplastic formulation (Maugin and Muschik, 1999). Perturbations to the local equilibrium assumption of the non-equilibrium thermodynamic theory of internal variables can lead to conditions of violation of smoothness on surfaces in a body, where one or more internal variables from the lower scale suffer jump discontinuities, owing to locally reaching a critical dissipation. In

140   a classical thermodynamic sense, this can be viewed as suddenly switching on a micro-engine somewhere in the system that disturbs the overall stress field. This is the physical reason for the formation of acceleration fronts, where the diffusive length-scales are linked to the convective velocity of the step function on dissipation waves. While fluid- and solid-wave phenomena occur when the above equation includes inertial forces, so-called 'acceleration waves'(Hill, 1962), caused by local surfaces of acceleration (see Fig. 4), can also occur in the creeping flow limit when no acceleration due to a (gravity) potential is present

145   and $\rho\mathbf{f} = 0$. These acceleration waves are defined as geometric surfaces (here assumed to be plane waves) that move relative to the material.

Acceleration waves can be described in two ways. One can use two coordinate systems, one for the reference state and one for the current state. A more elegant way is to consider convective coordinate systems by formulating the constitutive law in terms of stress-rate. For this we consider the space derivative normal to the moving wavefront (see Figure 4) indicated by $\frac{\partial}{\partial s}$.

150   Waves are travelling concerning a background Lagrangian moving material reference frame.

Considering the traction (load per unit area) in the direction normal to the wavefront as $\mathbf{F}$ and choosing the magnitude of the velocity of the moving wavefront as c, the jump condition indicated by the square Iverson brackets can be advected along c. This leads to Hadamard's jump condition where the true traction rate along the advected coordinates is:

$$\left[\dot{\mathbf{F}}\right] = -c\left[\frac{\partial\mathbf{F}}{\partial s}\right]. \tag{5}$$

155   Hadamard's jump condition applies to all internal variables and the acceleration across the wavefront is constrained by

$$[\rho\dot{\mathbf{v}}] = \left[\frac{\partial\mathbf{F}}{\partial s}\right]. \tag{6}$$
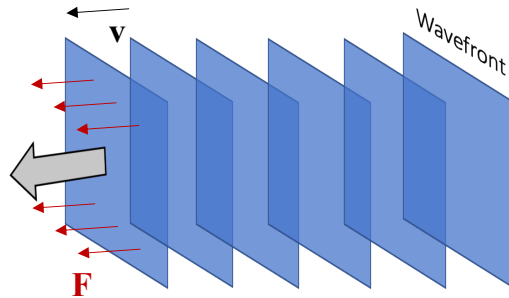
Figure 4. Acceleration waves can originate at a body surface when the existing internal stress gradient is dynamically incompatible with accelerations imposed on particles of the surface. A propagating plane-wave front is shown here for reference, but a plane-wave is not a necessary restriction. Across these surfaces particle accelerations and spatial gradients of velocity are momentarily discontinuous while the velocity itself is continuous.

Combining Eq. (5) and (6) we obtain

$$[\dot{\mathbf{F}}] + c[\rho\dot{\mathbf{v}}] = 0. \tag{7}$$

Substituting $\dot{\mathbf{v}} = -c\frac{\partial \mathbf{v}}{\partial s}$ into Eq. (7) we obtain

160 $$[\dot{\mathbf{F}}] = c^2 \left[\rho \frac{\partial \mathbf{v}}{\partial s}\right]. \tag{8}$$

Hill's formulation of acceleration waves in Eq. (8) expresses the energetics of the acceleration waves by the square of the material velocity c times the mass of the characteristic segment defined by $\frac{\partial \mathbf{v}}{\partial s}$. This provides a simple formulation where the energetics of the material is solely described by Eq. (1) and the mesoscale mass exchange rates on acceleration waves by Eq. (8). The material velocity c, being the velocity of acceleration waves becomes a material constant for the propagation of

165 acceleration waves. Acceleration waves form the basis of localization criteria in plasticity theory. The criterion for instability is derived from the equivalent theory in elastodynamics where for an elastoplastic body the acoustic tensor $\boldsymbol{\Gamma}$ is defined by

$$\boldsymbol{\Gamma} = \mathbf{n} \cdot \mathbf{C} \cdot \mathbf{n} \tag{9}$$

In elastodynamics, the eigenvalues of $\boldsymbol{\Gamma}$ divided by the mass density represent the square of the elastic wave propagation speed in the direction of the unit normal vector $\mathbf{n}$. In elasto-plasticity, the equivalent dynamic stability criterion is defined by Eq. (8)

170 which in terms of acoustic tensor implies that

$$\boldsymbol{\Gamma}\frac{\partial \mathbf{v}}{\partial s} = \rho c^2 \frac{\partial \mathbf{v}}{\partial s} \tag{10}$$

Dynamic system stability can be evaluated through assessing the eigenvalues of the acoustic tensor thus determining the speed of the acceleration waves which must be real and defined by the square root of the instantaneous modulus $\mathbf{C}$ divided by the instantaneous density ρ (Coleman and Gurtin, 1965). Mathematically, Eq. (2 - 4) can be represented by the addition of two

175 functions, a scalar field and the curl of a vector field. The former without curl or rotation identifies dissipative compressional P-waves and the latter features zero divergence and corresponds to isochoric sinistral and dextral dissipative shear S-waves.

These waves are interpreted as stationary (standing) waves when the determinant of the acoustic tensor and consequently the wave speed is zero,

$$det(\mathbf{\Gamma}) = 0 \tag{11}$$

180 which is the standard condition for localisation in plasticity theory (Vardoulakis and Sulem, 1995). Accordingly, the formation of localized shear-bands out of homogeneous plastic flow is assumed, when the velocity of the wavefront vanishes. Hill (1962) was discussing shear acceleration waves in an ideal linear, time-independent elasto-plastic material where two families of characteristics (dextral and sinistral slip lines) feature a jump in strain-rate at the wavefront accompanied by one in stress-rate (but not in stress). This in turn implies a related jump in stress gradient. Later work extended the theory to formulate

185 accelerations waves as the basis of modern criteria for localization in plastic media (Rudnicki and Rice, 1975; Rice, 1976). In those theories the possibility of volumetric acceleration waves was, however, neglected and volumetric deformation was parameterized by an empirical dilatancy angle. Another shortcoming of the localization criterion for the application to THMC instabilities is that it is not directly applicable to the rate-dependent elasto-viscoplastic case. The inclusion of rate effects implies a positive wave speed different from zero (Duszek-Perzyna and Perzyna, 1996). The *thermomechanics* approach (Jacquey and

190 Regenauer-Lieb, 2020) allows incorporation of a quasi-static wave speed related to the internal variable that quantifies the rate-dependence.

However, to date, no generally accepted localization criteria for the transition from a dynamic to quasistatic rate-dependent solution of Eq. (4) exists, although stationary and wave-like propagating localization phenomena for rate-sensitive materials (Barraclough et al., 2017) are observed in the laboratory and nature. The method of choice to date is to use all field equations

195 and perform a numerical stability analysis. A discussion on an extension to the above-discussed criterion has been presented recently (Pisanò and Prisco, 2016) and energy-based criteria that successfully model the adiabatic limit have been repeatedly revisited many times over the past 30 years (Paesold et al., 2016). The present approach provides an alternative path to systematically analyse the full system of field equations.

3.3 THMC acceleration waves

200 We assume creeping flow in Eq. (4), and there is, therefore, no effect of gravitational acceleration ($\rho \mathbf{F} = 0$). We will show that the meso-scale formalism identifies an alternate internal force density from within the considered material volume stemming from a local thermodynamic THMC force (e.g. ∇p). This internal force integrates over the accelerations $\mathbf{a_M}$ of the micro-processes inside the continuum element by multiplying them with the average volume density. These accelerations stem from dissipative mechanisms (e.g. volume changes by phase transitions, fracture, etc.) inside the representative volume element

205   (Hu et al., 2019). For critical conditions, they can cause acceleration waves propagating as creeping waves. Hadamard's jump conditions need to be extended for internal THMC variables μ such as temperature, porosity, permeability, viscosity, etc...

Hadamard's jump conditions state that if time derivatives ($\dot{\mathbf{F}}$, $\dot{\mathbf{v}}$, $\dot{\mu}$) and gradients $\nabla\mathbf{F}, \nabla\mathbf{v}, \nabla\mu$) have jump discontinuities across the wavefront then $\mathbf{F}, \mathbf{v}$ and μ are continuous functions of space. The compatibility condition relating jumps in rates of change of internal variables to jumps in gradients for all internal variables μ (Duszek-Perzyna and Perzyna, 1996) implying

210   that the jump in the gradient of pressure inside the acceleration wave is constrained by

$$[\nabla p] = -\frac{1}{c}[\dot{p}]. \tag{12}$$

Acceleration waves consider a step function (Eq. 5) where the stress-rate is discontinuous along the surface. The stress is, however, continuous across the wavefront and the stress self-diffusion coefficient is also constant outside of the wave. Therefore, for modelling acceleration waves in a homogeneous material we can simplify Eq. (1) further and assume constant bulk and

215   shear viscosity outside the wave and assume continuity of stress across the acceleration wave. Noting that the traction in the direction of the normal vector $\mathbf{n}$ on the acceleration wavefront is $\mathbf{F} = \mathbf{n} \cdot \boldsymbol{\sigma}$ it follows from Eq. (7) that the jump in stress-rate on the acceleration wave is (Duszek-Perzyna and Perzyna, 1996):

$$\mathbf{n} \cdot [\dot{\boldsymbol{\sigma}}] = -c[\rho\dot{\mathbf{v}}] \tag{13}$$

Substituting the stress-rate for the acceleration $\dot{\mathbf{v}}$ from Eq. (13) and the pressure rate for the gradient of pressure from Eq. (12)

220   and inserting the jump condition into Eq. (4) it follows that

$$\frac{1}{c}[\mathbf{n} \cdot [\dot{\boldsymbol{\sigma}}]] = -\frac{1}{c}[\dot{p}] - [\boldsymbol{C}\nabla(\dot{\boldsymbol{\epsilon}}')] - [\zeta\nabla\dot{\boldsymbol{\epsilon}}_{\mathbf{0}}] \tag{14}$$

If we define the magnitude of the wave speed in the normal reference system as $w = \mathbf{w} \cdot \mathbf{n}$, then $c = w - \mathbf{v} \cdot \mathbf{n}$ is the local particle velocity of THMC accelerations in the acceleration wave relative to the normal material velocity.

Eq. (14) allows us to draw some important conclusions for acceleration waves. (1) The first term on the right shows that the

225   pressure rate divided by the wave velocity or the equivalent gradient of pressure plays an important role in acceleration waves. (2) The second term on the right implies that gradients of deviatoric strain-rates are related to rate changes of the stiffness tensor as implied by the jump condition of the internal variable inside the propagating wave. Recall that the jump condition (Eq. 5 or 12) advects jumps in gradients of the internal variable around the propagating wavefront through a jump in the rate of change of the variable. (3) The last term implies that the same is true for the volumetric strain-rates and the rate of change

230   of bulk viscosity.

4   Multiscale cross-diffusion model

So far we have only discussed the mechanical reaction-diffusion equation, where the shear and bulk viscosities control the diffusion of stress. For the multiphysics implementation, it is convenient to think of diffusion of momentum and use the momentum diffusivity (kinematic viscosity) instead of the dynamic viscosity. We, therefore, denominate ζ_M as the volumetric

235   diffusion coefficient of pressure (kinematic viscosity). In the following, we first formulate the reaction-diffusion equation in a classical way. That is to say that meso-scale cross-diffusion effects are neglected. We identify THMC-Turing patterns as multiscale energy eigenstates of the reaction-diffusion equations thus characterizing Prigogine's dissipative structures if they emerge.

In these formulations, the viscous (M) mechanical pressure diffusion equation finds its counterparts in the equivalent thermal
240   (T) Fourier-, (H) Darcy- and (C) Fick's- diffusion laws where the diffusion coefficients are indicated by the associated THMC subscript. The corresponding reaction rates are the local hidden-variable reaction rate R_T, R_H, R_M and R_C, respectively. It is common practice to ignore the meso-scale cross-diffusion kinetics introduced in the classical theories of localisation. We emphasize therefore the difference between large-scale reaction rates R_i and meso-scale reaction rates r_i of the non-local theory which considers the important effect of cross-diffusion. The two rates are identical in the infinite time-scale limit as
245   cross-diffusion can be eliminated adiabatically (Biktashev and Tsyganov, 2016).

In the adiabatic limit we obtain similar reaction-diffusion equations across a vast range of THMC diffusion length scales as tabulated in Table 1. The reaction rates most often stem from different micro-processes at lower scale inside the considered continuum element which introduces cross-scale diffusion fluxes as shown in the next section. In order to generalize the

Table 1. Generalized Thermodynamic Fluxes and Forces in a THMC coupled system (1-D)

Type	*Force*	*Flux*	*reaction-diffusion equations*
T	$F_T = \nabla T$	$q_T = -\frac{DT}{Dt}$	$\frac{DT}{Dt} = \zeta_T \nabla^2 T + R_T$
H	$F_H = \nabla p_H$	$q_H = -\frac{Dp_H}{Dt}$	$-\frac{Dp_H}{Dt} = \zeta_H \nabla^2 p_H + \eta \dot{\epsilon}' - R_H$
M	$F_M = \nabla p_M$	$q_M = -\frac{Dp_M}{Dt}$	$-\frac{Dp_M}{Dt} = \zeta_M \nabla^2 p_M + \nabla(\boldsymbol{C}\dot{\boldsymbol{\epsilon}}') - R_M$
C	$F_C = \nabla C$	$q_C = -\frac{DC}{Dt}$	$\frac{DC}{Dt} = \zeta_C \nabla^2 C + R_C$

approach we propose that the composite multi-scale THMC wave operator $\hat{H}_{THMC}$ in Table 1 can be constructed through a
250   linear superposition characterized by

$$\hat{H}_{THMC} = -\zeta_i \sum_{i=1}^{N} \nabla_i^2, \tag{15}$$

where $\nabla_i^2 = \frac{\partial^2}{\partial x_i^2} + \frac{\partial^2}{\partial y_i^2} + \frac{\partial^2}{\partial z_i^2}$ and i refers to the individual thermodynamic THMC process. For the following discussion, we simplify further and neglect the deviatoric terms in Eq. 14 and retain only the scalar volumetric terms and reduce the equations to 1-D. This allows us to investigate the poorly known volumetric dissipative waves which must exist in addition
255   to the dissipative shear waves discussed by Hill (1962). To introduce the meso-scale considerations we identify wave scale reactive source terms r_T, r_H, r_M, r_C of the hidden variable rates R_T, R_H, R_M, R_C as the actual terms that trigger acceleration waves. These meso-scale source terms stem from a jump in the thermodynamic force (gradient of the variable) into a jump in the thermodynamic flux (rate of the variable, i.e. temperature, fluid, and solid pressure and concentration). The important

volumetric coupling is overlooked in the classical localisation theory (Rudnicki and Rice, 1975). The wave-scale source term

260 provides the convected pressure rate built up by internal accelerations. It relates to the local mass exchange processes according

to Eq. 8.

5 Cross-diffusion as a non-local theory for localisation

For evaluating the meso-scale mass exchange processes we use mixture theory (Hu et al., 2019). We consider two mass

fractions A and B for mass exchange denoted by the ith and j^{th} phase as an example. We identify $\dot{\xi}_i^{REV}$ as the large-scale

265 Representative Elementary Volume (REV) for averaging of mass transfer rate from the phases A to B where V_{REV}, V_A, V_B

denote the REV volume and the volume of the ith and j^{th} phase, respectively. $\dot{\xi}_i^{REV}$ defines the REV-scale averaging of the

mass exchange rate between the phases where the REV-scale source term of mass is obtained from the other species:

$$\dot{\xi}_i^{REV} = \frac{1}{V_{REV}} \int\limits_{V_{REV}} \dot{\xi}_j^{local} dV_{REV}, \tag{16a}$$

$$\dot{\xi}_j^{REV} = \frac{1}{V_{REV}} \int\limits_{V_{REV}} \dot{\xi}_i^{local} dV_{REV}, \tag{16b}$$

270 where $\dot{\xi}_i^{local}$ and $\dot{\xi}_j^{local}$ denotes the mass exchange rate from the A to B phase and vice-versa. In the meso-scale formalism

we need to consider information from the local scale processes in the THMC diffusion matrix and decompose the processes

leading to the local mass production $\dot{\xi}_i^{local}$ and $\dot{\xi}_j^{local}$. In order to specify this further we define the global volume fraction of

the A-phase as:

$$\phi = \frac{V_A}{V_{REV}} = 1 - \frac{V_B}{V_{REV}}, \tag{17}$$

275 Mass conservation at global scale for the phases A and B gives:

$$\frac{\partial[\rho_A V_A]}{\partial t} + \frac{\partial[\rho_A V_A v_A]}{\partial x} = \dot{\xi}_A V_{REV}, \tag{18a}$$

$$\frac{\partial[\rho_B V_B]}{\partial t} + \frac{\partial[\rho_B V_B v_B]}{\partial x} = \dot{\xi}_B V_{REV}. \tag{18b}$$

ρ_A and ρ_B identify the density of the respective phases, while v_A and v_B their velocities in the direction of x while $\dot{\xi}_A$ and $\dot{\xi}_B$

represent the volume averaged mass generation in the REV. Substituting Eq. 17 into Eq. 18 and eliminating V_{REV} gives

280

$$\frac{\partial[\rho_A \phi]}{\partial t} + \frac{\partial[\rho_A \phi v_A]}{\partial x} = \dot{\xi}_A^{REV}, \tag{19a}$$

$$\frac{\partial[\rho_B(1-\phi)]}{\partial t} + \frac{\partial[\rho_B(1-\phi)v_s]}{\partial x} = \dot{\xi}_B^{REV}. \tag{19b}$$

Repeating the same mass balance consideration for the local scale we obtain:

$$\dot{\xi}_B^{local} = \frac{\partial[\rho_B(1-\phi^{local})]}{\partial t} + \frac{\partial[\rho_B(1-\phi^{local})v_B]}{\partial x}, \tag{20a}$$

$$\dot{\xi}_A^{local} = \frac{\partial[\rho_A\phi^{local}]}{\partial t} + \frac{\partial[\rho_A\phi^{local}v_A]}{\partial x}, \tag{20b}$$

285 Substituting Eq. 20 into Eq. 19 via the upscaling law (Eq. 16), we have:

$$\frac{\partial[\rho_A\phi]}{\partial t} + \underbrace{\frac{\partial[\rho_A\phi v_A]}{\partial x}}_{Self-diffusion} + \underbrace{\frac{1}{V_{REV}}\int_{V_{REV}}\frac{\partial[\rho_B(1-\phi^{local})v_B]}{\partial x}dV_{REV}}_{Cross-diffusion}$$
$$= -\frac{1}{V_{REV}}\int_{V_{REV}}\frac{\partial[\rho_B(1-\phi^{local})]}{\partial t}, \tag{21a}$$

$$\frac{\partial[\rho_B(1-\phi)]}{\partial t} + \underbrace{\frac{\partial[\rho_B(1-\phi)v_B]}{\partial x}dV_{REV}}_{Self-diffusion} + \underbrace{\frac{1}{V_{REV}}\int_{V_{REV}}\frac{\partial[\rho_A\phi^{local}v_A]}{\partial x}dV_{REV}}_{Cross-diffusion}$$
$$= -\frac{1}{V_{REV}}\int_{V_{REV}}\frac{\partial[\rho_A\phi^{local}]}{\partial t}dV_{REV}, \tag{21b}$$

290 In a saturated porous medium, a straightforward interpretation of ρ_A and ρ_B may be the density of the fluid phase and that of the solid phase, respectively (Hu et al., 2019). The interpretation of the incorporation of the effects of chemical and thermal processes may not be as straightforward for the observer as they act via Eq. 15 as a linear convolution operation. If we interpret the time-domain convolution operation of THMC waves in the frequency domain, then the chemical and thermal waves can be seen as filters for HM coupling, sharpening or smoothing the waves. The interpretation of THMC waves in terms of a 295 sharpening or smoothing filter analogue is discussed in detail in part 2 (Regenauer-Lieb et al., 2020).

To illustrate the point of choosing a particular time-space scale of observation of THMC waves we first consider the simple homo-entropic flow assumption and choose a classical mechanics point of view. Density is then defined as a function of pressure, temperature, and chemical concentrations by the *Equation of State*. The coupling in Eq. 21 leads to the possible nucleation of Hydro-Mechanical cross-diffusion pressure waves (Hu et al., 2019). Considering that possible thermal processes, 300 ρ_A, and ρ_B, at the solid-fluid interface may be affected by the local temperature changes, we identify new time-dependent processes at the solid-fluid boundary. The process of heat transport sets two new internal timescales changing the fluid and solid pressure, respectively. Therefore, the thermal process acts as a 'convolution filter' added to the pressure evolution of each phase. Conversely, the pressure diffusion process in the solid and fluid phase triggers two additional timescales in the change of temperature. Now a 3×3 Thermo-Hydro-Mechanical cross-diffusion formulation can be obtained following the same steps 305 of upscaling from local to a global scale, and the additional 4 timescales correspond to the newly introduced 4 cross-diffusion

coefficients. One can arrive at a similar conclusion by considering the interplay between the evolution of pressure distribution and internal chemical reactions.

5.0.1 Formulation of the THMC cross-diffusion matrix

The concept of cross-diffusion is well known in chemistry. In a chemical system with just two species A and B, for instance,

310 cross-diffusion is the phenomenon, in which a flux of species A is induced by a gradient of species B (Vanag and Epstein, 2009). In more general THMC terms, cross-diffusion is the phenomenon where a gradient of one generalised thermodynamic force drives another generalised thermodynamic flux. Staying with the chemical example of species A and B, we have in 1-D:

$$\frac{\partial C_A}{\partial t} = \zeta_A \frac{\partial^2 C_A}{\partial x^2} + L_{AB} \frac{\partial^2 C_B}{\partial x^2} + r_B$$

$$\frac{\partial C_B}{\partial t} = \zeta_B \frac{\partial^2 C_B}{\partial x^2} + L_{BA} \frac{\partial^2 C_A}{\partial x^2} + r_A. \tag{22}$$

where r_A and r_B are the local source terms using the mesoscopic self-diffusion and cross-diffusion decomposition in Eq. (21).

315 Following Eq. (15) we can now generalize (22) to include the full cascade of internal accelerations through multiscale coupling. Cross-diffusion allows coupling of accelerations from one classical REV-scale reaction-diffusion system, defined by the (self-)diffusive length scale $\sqrt{\zeta_{(T,H,M,C)}t}$, to another. These cross-diffusion coefficients link the gradient of a thermodynamic force C_j of one THMC process to the flux of another kind. This allows the definition of a fully populated diffusion matrix as in:

$$\frac{D\mathbf{C}}{Dt} = \begin{bmatrix} \zeta_T & L_{TH} & L_{TM} & L_{TC} \\ L_{HT} & \zeta_H & L_{HM} & L_{HC} \\ L_{MT} & L_{MH} & \zeta_M & L_{MC} \\ L_{CT} & L_{CH} & L_{CM} & \zeta_C \end{bmatrix} \nabla^2 \mathbf{C} + r_i. \tag{23}$$

320 The cross-diffusion processes formulate the link between different THMC processes. The cross-diffusion coefficients thereby introduce new cross-scale coupling length and the time scales and are often much smaller than the self-diffusion scales. This is not always the case (Manning, 1970). Hu et al. (2019) show normal examples where cross-diffusion length/time scales are much smaller than the self-diffusion length scales.

5.0.2 Criterion for nucleation of cross-diffusion Waves

325 A detailed discussion of the criterion for nucleation of cross-diffusion waves and their waveforms can be found in Tsyganov and Biktashev (Tsyganov and Biktashev, 2014). Here, we first summarize the basic method that is well established in the fields of mathematical biology and chemistry and follow on with a discussion of other communities, where the phenomenon of cross-diffusion waves is well-documented under different names.

The criterion for nucleation of cross-diffusion waves relies on assessing the dispersion relation of the eigenvalues of the char-

330 acteristic matrix of a perturbed cross-diffusion-reaction equation (Vanag and Epstein, 2009). The eigenvalues are functions of

the square of the wavenumber of the perturbed state and identify the growth rate of the perturbations. This approach for deriving the mathematical criterion for nucleation of acceleration waves is hence evaluated from a small plane-wave ϵ-perturbation of Eq. (23) with

$$\tilde{\mathbf{C}}(x,t) = \mathbf{C}_0(1+\epsilon)\mathrm{e}^{\lambda t + i(kx)} \tag{24}$$

335   The characteristic matrix of the thus perturbed Eq. (23) allows assessing the stability of the system. Accordingly, all eigenvalues of the characteristic matrix must be real and positive, and hence the determinant of the matrix must be larger than zero. For determinants smaller than zero, cross-diffusion waves are expected to propagate as quasi-solitons (Tsyganov and Biktashev, 2014). A worked example for hydromechanical cross-diffusion waves can be found in Hu et al. (2019).

6   Soliton versus quasi-soliton solutions

340   Since cross-diffusion waves in geomaterials are largely unexplored due to the extreme length and time scales encountered in a geosystem, an appreciation of their complex characteristics can be obtained from mathematically similar systems such as waves in oceans, Lasers, and ice. There is an important difference between solitonic waves and quasi-solitonic cross-diffusion waves. We follow Zakharov et al.'s (Zakharov and Kuznetsov, 1998) definition of solitons and quasi-solitons and identify solutions to the perturbed Eq. 24 of the type:

345   $$\psi(x,t) = \beta(x - \mathbf{v}t)e^{i\Omega t}, \tag{25}$$

as solitons when the wave amplitude $|\psi(x,t)| = |\beta(x - \mathbf{v}t)|$ propagates without change of form and $\mathbf{v}$ and Ω are constants. Quasi-solitons appear as non-local solutions to Eq. (24) if localized coherent structures defined by true soliton solutions cannot be formed for any type of non-linearity. In the context of the cross-diffusion waves for hydro-poro-mechanical coupling (Hu et al., 2019) real stationary solitons, which propagate with a constant velocity without changing their form, are exact solutions

350   of the Korteweg-deVries equation (Regenauer-Lieb et al., 2013; Veveakis and Regenauer-Lieb, 2015). They depend on the fluid- and solid self-diffusion coefficients only (Veveakis and Regenauer-Lieb, 2015). Cross-diffusion waves are quasi-solitons where the two additional cross-diffusion coefficients cannot be eliminated (Hu et al., 2019). These additional time-dependent properties lead to interesting dynamics.

    Following dynamic properties of quasi-solitons have been identified (Zakharov et al., 2004): Quasi-solitons live only for

355   a finite time and can be compared to unstable particles in nuclear physics. Unlike true solitons, quasi-solitons loose energy through their oscillatory tails which can have different wavenumbers in the forward and backward direction of their motion. If the amplitudes of the tails are small, quasi-solitons can be treated as slowly decaying real solitons which lose their energy by radiating quasi-monochromatic waves with wavenumber k_0 in the backward direction.

    The discrete particle-like behaviour can be explained by their unusual dispersion relation. Quasi-solitons travel with a con-

360   stant group velocity ω'. When their phase velocity $\omega(k)/k$ exhibits a local minimum at a nonzero wavenumber a gap in the spectrum $\omega(k)$ appears. According to Zakharov et al. (2004), this peculiar discretization of wave energy has been noticed in

many disciplines. Different nomenclatures of quasi-solitons have been adopted. In the theoretical physics community, they have been attributed to Cherenkov radiation. In the ice-wave community, they have been called ice-waves with decaying oscillations and in shallow water theory, they have been identified as capillary-gravity waves. If the amplitudes of the quasi-solitons

365 are small and their velocities are close, they obey the non-linear Schrödinger equation and their interaction is elastic. However, the stability and the interaction of large amplitude quasi-solitons are still open questions that cannot be solved analytically. Quasi-solitons move with different velocities and can lead to quasi-solitonic turbulence? (Zakharov et al., 2004) when they collide with each other.

In photonics, optical turbulence in the form of sporadic bursts of light (Hammani et al., 2010), have been observed upon the

370 collision of quasi-solitons. In water waves, the same phenomenon is known as 'rogue waves' that seem to appear from nowhere (Akhmediev et al., 2009). Their physics relies on the unusual non-local energetics of quasi-solitons that can pump energy from the environment to provide a quasi-stationary transport of wave energy from large to small scales. Earlier, we have introduced a simple 'convolution filter' interpretation of THMC coupling. In this sense, the interaction of THMC-waves may be seen as an extreme form of sharpening filter that can generate rogue waves.

375 The independent choice of a reference system such as discussed in the convolution filter analogy also applies to the energy carried by the waves. If we choose for instance an observer of hydro-mechanical waves, the inverse energy cascade from THMC wave action from small to large-scale and the direct energy cascade from large to small-scales (Zakharov et al., 2004) allows the identification of rogue waves, if they occur. The phenomenon of the collision, merging, and the collapse of quasi-solitons may provide a mechanism for a bi-directional THMC energy cascade that leads to earthquakes as a form of solid-state

380 turbulence as discussed in the application in part 2 (Regenauer-Lieb et al., 2020).

7 Conclusions

We have presented a simple non-local theory for the multi-physics of material instabilities and shown its link to classical theories of localisation instabilities in continuum mechanics. The approach reveals that instabilities based on the volumetric response of the material are fundamentally important but have been overlooked in earlier theories. We have also shown

385 that incompatibilities of meso-scale accelerations with the overall stress field lead to the nucleation of cross-diffusion waves which travel in an unstable particle-like state with characteristic material velocities c defined by the competition of meso-scale reaction-diffusion processes at the propagating wavefront. These velocities characterise the progress of internal material timescales for the formation of multiscale space/time dissipative structures and are characteristic properties for the dynamic behaviour of a given material. These internal material clocks are here introduced as a multiscale THMC cascade for coupling

390 the physics of the very small to the very large.

Cross-diffusion waves have first been discovered in photonics where they show anomalous dispersion patterns that, unlike solitons radiate energy in the form of oscillatory (Cherenkov)-tails (Zakharov and Kuznetsov, 1998; Paschotta, 2008). This unusual energy radiation property differentiates them from solitons as quasi-solitons. Since they assume an unstable particle-like state, the reflections and collisions, when they happen, can lead to a variety of responses (Biktashev and Tsyganov,

395 2016; Zakharov et al., 2004; Lioubashevski et al., 1996). Despite their nucleation through discrete internal micro-dissipative
mechanisms, cross-diffusional waves also show proper soliton wave-like behaviour and can penetrate through each other and
reflect from boundaries. However, unlike true solitons, their amplitude and speed are not controlled by initial conditions but by
material properties (Tsyganov and Biktashev, 2014). The effect of cross-diffusion is to trigger cross-diffusion waves for critical
conditions. They form by THMC-feedback as discrete material instabilities which can be either observed as a local, discrete
400 failure or as damage waves. We have shown that cross-diffusion waves in THMC systems can be decomposed into cross-
diffusional S- and P- acceleration waves and have discussed a THMC multiphysics implementation, where cross-diffusion
waves appear as quasi-soliton waves for critical conditions identified from a perturbed Eq. (23). Their role in pumping wave
energy over multiple length-scales through multiphysics THMC-feedbacks can cause 'solid-state turbulence'. This may be
considered a potential source mechanism for the nucleation of earthquakes. Their unstable non-local nature and their capability
405 to focus energy from the large-scale to feed local scale 'rogue waves' (Zakharov et al., 2004; Akhmediev et al., 2009) is well
documented in photonics (Solli et al., 2007) and shallow water theory (Akhmediev et al., 2009).

8   Acknowledgments

This work was supported by the Australian Research Council (ARC DP170104550, DP170104557) and the strategic SPF01
fund of UNSW, Sydney. We would also like to acknowledge constructive feedback of Mike Trefry.

References

Akhmediev, N., Soto-Crespo, J. M., and Ankiewicz, A.: Extreme waves that appear from nowhere: On the nature of rogue waves, Physics Letters A, 373, 2137–2145, https://doi.org/https://doi.org/10.1016/j.physleta.2009.04.023, http://www.sciencedirect.com/science/article/pii/S0375960109004939, 2009.

Alevizos, S., Poulet, T., Sari, M., Lesueur, M., Regenauer-Lieb, K., and Veveakis, M.: A Framework for Fracture Network Formation in Overpressurised Impermeable Shale: Deformability Versus Diagenesis, Rock Mechanics and Rock Engineering, 50, 689–703, 2017.

Ball, P.: Pattern Formation in Nature: Physical Constraints and Self-Organising Characteristics, Architectural Design, 82, 22–27, https://doi.org/10.1002/ad.1375, https://doi.org/10.1002/ad.1375, 2012.

Barraclough, T. W., Blackford, J. R., Liebenstein, S., Sandfeld, S., Stratford, T. J., Weinländer, G., and Zaiser, M.: Propagating compaction bands in confined compression of snow, Nature Physics, 13, 272–275, https://doi.org/10.1038/nphys3966, https://doi.org/10.1038/nphys3966, 2017.

Biktashev, V. N. and Tsyganov, M. A.: Quasisolitons in self-diffusive excitable systems, or Why asymmetric diffusivity obeys the Second Law, Scientific Reports, 6, 30 879, https://doi.org/10.1038/srep30879 https://www.nature.com/articles/srep30879#supplementary-information, 2016.

Chen, X., Roshan, H., Lv, A., Manman, H., and Regenauer-Lieb, K.: The dynamic evolution of compaction bands in highly porous carbonates: The role of local heterogeneity for nucleation and propagation, Progress in Earth and Planetary Sciences, p. submitted, 2020.

Coleman, B. D. and Gurtin, M. E.: Thermodynamics and the Velocity of General Acceleration Waves, in: Wave Propagation in Dissipative Materials, edited by Coleman, B. D., Gurtin, M. E., Herrera R, I., and Truesdell, C., pp. 83–104, Springer Berlin Heidelberg, 1965.

Coleman, B. D., Gurtin, M. H., Herrera R, I., and Truesdell, A. H.: Wave Propagation in Dissipative Materials, Springer-Verlag, Berlin, 1965.

deGroot, S. R.: Non-equilibrium thermodynamics, Amsterdam, North-Holland Pub. Co. New York, Interscience Publishers, Amsterdam, New York, 1962.

Dewers, T. and Ortoleva, P.: Geochemical self-organization III, A mechano-chemical model of metamorphic differentiation, American Journal of Science, 290, 473–521, https://doi.org/10.2475/ajs.290.5.473, 1990.

Duszek-Perzyna, M. and Perzyna, P.: Adiabatic shear band localization of inelastic single crystals in symmetric double-slip process, Archive of Applied Mechanics, 66, 369–384, 1996.

Einav, I. and Guillard, F.: Tracking time with ricequakes in partially soaked brittle porous media, Science Advances, 4, eaat6961, https://doi.org/10.1126/sciadv.aat6961, https://advances.sciencemag.org/content/advances/4/10/eaat6961.full.pdf, 2018.

Grigoli, F., Cesca, S., Rinaldi, A. P., Manconi, A., López-Comino, J. A., Clinton, J. F., Westaway, R., Cauzzi, C., Dahm, T., and Wiemer, S.: The November 2017 5.5 Pohang earthquake: A possible case of induced seismicity in South Korea, Science, 360, 1003, https://doi.org/10.1126/science.aat2010, http://science.sciencemag.org/content/360/6392/1003.abstract, 2018.

Guillard, F., Golshan, P., Shen, L., Valdes, J. R., and Einav, I.: Dynamic patterns of compaction in brittle porous media, Nature Physics, 11, 835–838, 2015.

Hammani, K., Kibler, B., Finot, C., and Picozzi, A.: Emergence of rogue waves from optical turbulence, in: Nonlinear Photonics, vol. hal-00469974, p. NMA5, HAL archives ouvertes, 2010.

Heilmann, I. T., Thygesen, U. H., and Soerensen, M. P.: Spatio-temporal pattern formation in predator-prey systems with fitness taxis, Ecological Complexity, 34, 44–57, https://doi.org/https://doi.org/10.1016/j.ecocom.2018.04.003, http://www.sciencedirect.com/science/article/pii/S1476945X1830062X, 2018.

Hill, R.: Acceleration waves in solids, Journal of the Mechanics and Physics of Solids, 10, 1–16, https://doi.org/https://doi.org/10.1016/0022-5096(62)90024-8, 1962.

Hu, M., Schrank, C., and Regenauer-Lieb, K.: Cross-diffusion Waves in Hydro-Poro-Mechanics, Journal of the Mechanics and Physics of Solids, https://doi.org/https://doi.org/10.1016/j.jmps.2019.05.015, http://www.sciencedirect.com/science/article/pii/S0022509619301541, 2019.

Jacquey, A. and Regenauer-Lieb, K.: Thermomechanics for geological, civil engineering and geodynamic applications, Solid Earth, Geoproc Conference 2019, submitted, 2020.

L'Heureux, I.: Self-organized rhythmic patterns in geochemical systems, Philosophical Transactions of the Royal Society A: Mathematical, Physical and Engineering Sciences, 371, 20120 356, https://doi.org/10.1098/rsta.2012.0356, https://doi.org/10.1098/rsta.2012.0356, 2013.

Lioubashevski, O., Arbell, H., and Fineberg, J.: Dissipative Solitary States in Driven Surface Waves, Phys. Rev. Lett., 76, 3959–3962, https://doi.org/10.1103/PhysRevLett.76.3959, https://link.aps.org/doi/10.1103/PhysRevLett.76.3959, 1996.

L'Heureux, I.: Diagenetic Self-Organization and Stochastic Resonance in a Model of Limestone-Marl Sequences, Geofluids, 2018, Article ID 4968 315, https://doi.org/doi.org/10.1155/2018/4968315, 2018.

Manning, J. R.: Cross terms in the thermodynamic diffusion equations for multicomponent alloys, Metallurgical and Materials Transactions B, 1, 499–505, https://doi.org/10.1007/BF02811561, https://doi.org/10.1007/BF02811561, 1970.

Maugin, G. and Muschik, W.: THERMODYNAMICS WITH INTERNAL VARIABLES, vol. Volume 27 of *World Scientific Series on Nonlinear Science Series A*, pp. 77–105, WORLD SCIENTIFIC, https://doi.org/doi:10.1142/9789812796271_0004 10.1142/9789812796271_0004, https://doi.org/10.1142/9789812796271_0004, 1999.

Ortoleva, P. J.: Self-Organization and Nonlinear Dynamics in Sedimentary Basins, Philosophical Transactions of the Royal Society of London Series a-Mathematical Physical and Engineering Sciences, 344, 171–179, file://Dl/pdf/ptrs_1993_344_171.pdf, 1993.

Ortoleva, P. J.: Geochemical Self-Organization, Oxford University Press, New,York, 1994.

Paesold, M., Bassom, A., Regenauer-Lieb, K., and Veveakis, M.: Conditions for the localisation of plastic deformation in temperature sensitive viscoplastic materials, Journal of Mechanics of Materials and Structures, 11, 113–136, 2016.

Paschotta, R.: Quasi-Soliton pulses, Wiley-VCH, 1st edition october 2008 edn., 2008.

Pisanò, F. and Prisco, C. d.: A stability criterion for elasto-viscoplastic constitutive relationships, International Journal for Numerical and Analytical Methods in Geomechanics, 40, 141–156, https://doi.org/10.1002/nag.2395, https://doi.org/10.1002/nag.2395, 2016.

Regenauer-Lieb, K., Veveakis, M., Poulet, T., Wellmann, F., Karrech, A., Liu, J., Hauser, J., Schrank, C., Gaede, O., and Fusseis, F.: Multiscale coupling and multiphysics approaches in earth sciences: Applications, Journal of Coupled Systems and Multiscale Dynamics, 1, 2330–152X/2013/001/042, https://doi.org/10.1166/jcsmd.2013.1021, 2013.

Regenauer-Lieb, K., Poulet, T., and Veveakis, M.: A novel wave-mechanics approach for fluid flow in unconventional resources, The Leading Edge, 35, 90–97, 2016.

Regenauer-Lieb, K., Hu, M., Schrank, C., Chen, X., Pena Clavijo, S., Kelka, U., Karrech, A., Gaede, O., Blach, T., Roshan, H., and Jacquey, A.: Cross-Diffusion Waves as a trigger for Multiscale, Multi-Physics Instabilities: Application to Earthquake Instabilities, Solid Earth, submitted, 2020.

Rice, J. R.: The localization of plastic deformation, pp. 207–220, North-Holland, Amsterdam, 1976.

Rudnicki, J. and Rice, J.: Conditions for the localization of deformation in pressure sensitive dilatant materials., J. Mech. Phys. Solids, 23, 371–394, 1975.

Sanderson, A. R., Kirby, R. M., Johnson, C. R., and Yang, L.: Advanced Reaction-Diffusion Models for Texture Synthesis, Journal of
    Graphics Tools, 11, 47–71, https://doi.org/10.1080/2151237X.2006.10129222, https://doi.org/10.1080/2151237X.2006.10129222, 2006.

Solli, D. R., Ropers, C., Koonath, P., and Jalali, B.: Optical waves, Nature, 450, 1054, https://doi.org/10.1038/nature06402, https://doi.org/
    10.1038/nature06402, 2007.

Tsyganov, M. A. and Biktashev, V. N.: Classification of wave regimes in excitable systems with linear cross diffusion, Phys. Rev. E, 90,
    062 912, https://doi.org/10.1103/PhysRevE.90.062912, 2014.

Turing, Alan, M.: The chemical basis of morphogenesis, Philosophical Transactions of the Royal Society of London. Series B, Biological
    Sciences, 237, 37–72, https://doi.org/10.1098/rstb.1952.0012, https://doi.org/10.1098/rstb.1952.0012, 1952.

Vanag, V. K. and Epstein, I. R.: Cross-diffusion and pattern formation in reaction–diffusion systems, Physical Chemistry Chemical Physics,
    11, 897–912, https://doi.org/10.1039/B813825G, 2009.

Vardoulakis, I. and Sulem, J.: Bifurcation Analysis in Geomechanics, Blankie Acc. and Professional, Glasgow, 1995.

Vasil'ev, V. A.: Autowave processes in distributed kinetic systems, Soviet Physics Uspekhi, 22, 615–639,
    https://doi.org/10.1070/PU1979v022n08ABEH005591, 1979.

Veveakis, E. and Regenauer-Lieb, K.: Cnoidal waves in solids, Journal of the Mechanics and Physics of Solids, 78, 231–248, 2015.

Zakharov, V., Dias, F., and Pushkarev, A.: One-dimensional wave turbulence, Physics Reports, 398, 1–65,
    https://doi.org/10.1016/j.physrep.2004.04.002, https://www.scopus.com/inward/record.uri?eid=2-s2.0-3042652794&doi=10.1016%
    2fj.physrep.2004.04.002&partnerID=40&md5=eb7132cda7a9fd12d042f52cb4a8097d, 2004.

Zakharov, V. E. and Kuznetsov, E. A.: Optical solitons and quasisolitons, Journal of Experimental and Theoretical Physics, 86, 1035–1046,
    https://doi.org/10.1134/1.558551, https://doi.org/10.1134/1.558551, 1998.

Zemskov, E. P., Tsyganov, M. A., and Horsthemke, W.: Oscillatory pulses and wave trains in a bistable reaction-diffusion system with cross
    diffusion, Physical Review E, 95, 012 203, https://doi.org/10.1103/PhysRevE.95.012203, https://link.aps.org/doi/10.1103/PhysRevE.95.
    012203, 2017.